



Enhancement of Naphthalene Degradation by a Sequential Sulfate Injection Scenario in a (Semi)-Arid Coastal Soil: a Flow-Through Reactor Experiment

Saeid Shafieiyoun · Riyadh I. Al-Raoush · Stephane K. Ngueleu · Fereidoun Rezanezhad · Philippe Van Cappellen

Received: 20 January 2020 / Accepted: 23 June 2020 / Published online: 31 July 2020
© The Author(s) 2020

Abstract Engineered sulfate injection has been introduced as an effective technology to enhance the remediation of soil and groundwater contaminated by petroleum hydrocarbons. While some studies indicate that sulfate injection is a promising method for the treatment of hydrocarbon-contaminated subsurface systems, its application in the brackish soil environments is unknown. In this study, we explored related geochemical indicators along with soil adsorption and dissolved phase concentrations to provide an improved understanding of the hydrocarbon-contaminated subsurface responses to the sulfate injection in brackish environments. A series of flow-through experiments representing in situ groundwater anaerobic bioremediation were conducted and two sulfate injection episodes were applied to examine the degradation of dissolved naphthalene under low salinity and brackish conditions. As opposed to the substantial body of previous studies that salinity restricts biodegradation, the results from

this study showed that naphthalene anaerobic degradation was more stable once the salinity was as high as that at the sampling location in the coastal brackish environment. While increasing naphthalene concentration from 4 to 12 mg L⁻¹ did not limit biodegradation efficiency under brackish condition similar to the sampling location, it adversely restricted the developed reducing conditions and biodegradation process under low salinity conditions. This highlights the adaption of the microbial communities within the soil to the brackish environment at the sampling location suggesting that changing the salinity during engineered sulfate application can make the remediation process more susceptible against the environmental stresses and substrate toxicity. The results of this study provide insight into the engineered sulfate application as a remediation strategy for potential removal of dissolved naphthalene from the contaminated brackish groundwater.

Electronic supplementary material The online version of this article (<https://doi.org/10.1007/s11270-020-04725-5>) contains supplementary material, which is available to authorized users.

S. Shafieiyoun · R. I. Al-Raoush (✉) · S. K. Ngueleu
Department of Civil and Architectural Engineering, College of Engineering, Qatar University, PO Box 2713, Doha, Qatar
e-mail: riyadh@qu.edu.qa

S. K. Ngueleu · F. Rezanezhad · P. Van Cappellen
Ecohydrology Research Group and Water Institute, Department of Earth and Environmental Sciences, University of Waterloo, 200 University Avenue West, Waterloo, Ontario N2L 3G1, Canada

Keywords Naphthalene degradation · Sulfate injection · Hydrocarbon-contaminated groundwater · Brackish groundwater

1 Introduction

Soil and groundwater contamination resulting from petroleum hydrocarbons is one of the major environmental issues. Due to low solubility of petroleum hydrocarbons and mass transfer limitations, these contaminants often persist in subsurface systems as a separate non-aqueous

phase liquid (NAPL) (Mercer and Cohen 1990; Al-Raoush 2014; Shafieiyoum et al. 2018). Bioremediation is an effective treatment remedy in terms of cost, efficiency, safety, and application simplicity (Jain et al. 2011; Varjani 2017). While natural attenuation is the most common biological remedy applied in the contaminated sites (Megharaj et al. 2011; Perelo 2010), the biodegradation process can be hindered due to lack of essential nutrients and/or terminal electron acceptors (Lovley et al. 1995; Vallejo et al. 2001; Nguieu et al. 2019). Hence, supplying the electron acceptors and essential nutrients in the contaminated subsurface systems has been proposed to enhance the indigenous microbial activities (Kauppi et al. 2011; Müller et al. 2017; Simpanen et al. 2016; Wei et al. 2018).

Field scale application of electron acceptors (e.g., sulfate) can be conducted by single or multiple injection of substances (Lebkowska et al. 2011), but the processes are still associated with high uncertainties (Henry 2010). For example, while some studies indicate that supplying the electron acceptors and essential nutrients can be a promising method (Cunningham et al. 2001; Godleads et al. 2015; Simpanen et al. 2016; Suthersan et al. 2011), Bento et al. (2005) showed that natural attenuation is more effective compared to nutrient addition.

Anaerobic biodegradation is the dominant metabolic process in the petroleum-contaminated subsurface systems since the dissolved oxygen (DO) can be depleted rapidly due to aerobic degradation of organic compounds (Anderson and Lovley 1997; Ning et al. 2018; Perelo 2010). The previous field and laboratory experiments have shown that hydrocarbons can be degraded under anaerobic conditions in the presence of various electron acceptors such as nitrate (Burland and Edwards 1999), sulfate (Lovley et al. 1995; Thierrin et al. 1993; Wei et al. 2018), and iron ions (Coates et al. 1996; Lovley et al. 1989; Lovley and Lonergan 1990). Sulfate reduction is one of the most favorable anaerobic processes in the subsurface systems performed by a wide range of microbes known as sulfate-reducing bacteria (SRB). SRB degrade organics as their carbon source that makes them suitable organisms for the bioremediation of contaminated groundwater (Miao et al. 2012).

Many of the petroleum hydrocarbons which are dominant in the contaminated subsurface systems can be anaerobically degraded under sulfate-reducing conditions (Gan et al. 2009; Meckenstock et al. 2016). While biodegradation of monoaromatic hydrocarbons such as benzene, toluene, ethylbenzene, and xylene (BTEX) is well elaborated

in previous studies (Boll et al. 2002; Fuchs et al. 2011), for the polycyclic aromatic hydrocarbon (PAH), it is not well understood (Meckenstock et al. 2016). The biodegradation of PAH has been reported to be slow probably due to low energy conservation and slow growth of bacteria (Meckenstock et al. 2016). For example, anaerobic degradation of naphthalene under sulfate-reducing condition has been reported previously (Galushko et al. 1999; Musat et al. 2009), but Thierrin et al. (1993) demonstrated that naphthalene had the lowest degradation rate between dissolved BTEX, trimethylbenzenes, and naphthalene under sulfate-reducing conditions. Sulfate reduction leads to decrease in redox potential and also production of reactive sulfide which is toxic and thus not desirable; however, sulfide can be precipitated as iron sulfide depending on the natural availability of iron in the aquifer (Acton and Barker 1992). In addition, hydrocarbon mineralization under sulfate-reducing conditions yields bicarbonate which gives rise in alkalinity and pH as well as dissolved inorganic carbon (DIC) in the groundwater (Davis et al. 1999; Suthersan et al. 2011; Wei et al. 2018). All these effects are considered as geochemical indicators of the activity of SRB in the subsurface systems.

Biodegradation is highly sensitive to environmental conditions such as background conditions and bioavailability of the contaminants, electron acceptor accessibility, pH, temperature, soil moisture, and salinity (Meckenstock et al. 2016; Megharaj et al. 2011; Varjani 2017) that need to be considered during the design and implementation of bioremediation strategies. For example, coastal zones and marine sediments are susceptible to be contaminated by industrial activities such as crude oil production (Rushdi et al. 2017) and their salinity can restrict the type of applied bioremediation techniques (Perelo 2010). Previous studies considering the effect of salinity on the biodegradation of petroleum hydrocarbons have mostly focused on the organisms and mechanisms in which organic compounds can be degraded and in general indicate that salinity can inhibit the microbial activities (Abed et al. 2015; Ajisebutu 1988; Brusa et al. 2001; María Piedad Díaz et al. 2000; Mille et al. 1991; Thamer et al. 2013; Ward and Brock 1978). Abed et al. (2015) performed a series of microcosm tests and indicated that the microbial community significantly changed after an increase of the salinity from 2 to 7% NaCl. In addition, bacterial respiration and organic mineralization were significantly reduced as the salinity increased. Garcia-Blanco et al. (2001) in a microcosm study indicated that the lack of oxygen may limit the hydrocarbon biodegradation in a simulated tidal salt marsh

environment. Mille et al. (Mille et al. 1991) reported that crude oil biodegradation by a mixed aerobic bacterial community isolated from a marine sediment was enhanced to a maximum NaCl concentration of 0.4 mol L^{-1} and then decreased for the higher concentrations. Rhykerd et al. (1995) investigated the influence of salinity on the bioremediation of petroleum-contaminated soils using a series of aerobic batch experiments amended by NaCl salt. Their results indicated that after 80 days, the mineralized oil in sandy-clay slurry systems with electrical conductivities (EC) of 0, 40, 120, and 200 mS cm^{-1} was 40, 37, 30, and 20%, respectively.

While these studies provide valuable information, isolated microbial studies and batch systems result in the most optimistic conditions, and application of the biological methods in the petroleum-contaminated sites with different levels of salinity requires further investigations, which are more representative of anaerobic subsurface conditions. Diverse ranges of active SRB have been shown in the anaerobic saline and brackish environments (Ben-Dov et al. 2009; Capone and Kiene 1988; Caumette 1986; Foti et al. 2007; Laanbroek and Pfennig 1981), which can be employed to degrade organic contaminants under anaerobic subsurface conditions. Oxidation of fatty acids by substantial sulfate-reducing rates was also reported by Foti et al. (2007) in soda lakes under highly alkaline and saline conditions. Laanbroek and Pfennig (1981) also identified that acetate and propionate were degraded in freshwater and brackish water under sulfate-reducing condition. Capone and Kiene (1988) reported that differences of the chemical environments between freshwater, brackish water, and marine systems result in distinct microbial activities in each system. However, to the best of our knowledge, there is no study that explores the effects of salinity on the engineered sulfate injection as a remediation method in the organic contaminated subsurface systems.

Shafieiyoun et al. (2020) in a series of flow-through experiments showed that the overall effects of salinity on organic compounds degradation under sulfate-reducing conditions are affected by substrate interactions and NAPL composition. The goal of this study was to delineate the net influence of salinity on the remediation of a hydrocarbon plume by a sequential sulfate injection scenario in a (semi)-arid brackish coastal soil environment, and hence, a single organic contaminant was chosen for the purpose of this evaluation. Using a series of flow-through experiments, we

monitored the development of reducing condition as well as related geochemical indicators (i.e., pH, redox potential (Eh), DIC, EC) to evaluate hydrocarbon-contaminated subsurface responses to the engineered sulfate injection in the brackish water environments. Naphthalene, a dominant PAH in many of the petroleum-contaminated sites (Birak and Miller 2009), was chosen as the dissolved hydrocarbon and the influence of sequential multiple injection of sulfate on two different dissolved naphthalene concentrations were tested under two salinity conditions representing fresh water and brackish water conditions.

2 Materials and Methods

2.1 Field Site and Soil Sampling

Since the objective of this study was to investigate the effect of salinity on the performance of sulfate injection as a remediation technology, a controlled condition with a predetermined organic concentration was intended. Hence, non-contaminated soil samples were employed and a constant dissolved naphthalene concentration was injected during each sulfate injection episode. In fact, the focus of this study was to apply remediation practices on the contaminated plume downgradient of the source zone and it was not intended to evaluate mass removal in the source zone. Soil samples were initially tested by gas chromatography analyses to ensure not impacted by any organic contaminants.

Soil samples were collected from a shoreline area known as Sumaysimah beach in the State of Qatar ($25^{\circ} 34' 26.61'' \text{ N}$; $51^{\circ} 29' 18.77'' \text{ E}$). The samples were collected between depths of 0 to 10 cm below the ground surface and above the groundwater table. To collect undisturbed soil samples, a shuttle corer was used. Plexiglas reactor tubes (10 cm length and 4.7 cm inner diameter) were placed inside the shuttle corer and then gently pushed to the ground at the sampling location. Hence, the Plexiglas tube was filled by undisturbed soil core sample (for more details, please see Pallud et al. 2007). Following sampling, Plexiglas tubes were gently and quickly capped to ensure the soil matrix will not be affected, then wrapped by aluminum foil and placed in a cooler and shipped to the laboratory at University of Waterloo.

The soil texture was silty-sandy and calcite is the main mineral in this soil (Ngueleu et al. 2018; Shomar 2015; Yigiterhan et al. 2018). The mechanical sieving analyses

showed that specific particle diameters equivalent to 10 and 60% passing (d_{10} and d_{60}) were 0.11 and 0.58 mm, respectively, and the particle density of the soil was 2.72 kg L^{-1} (Ngueleu et al. 2018). Pore water pH and EC at the sampling location in the coastal soil environment were ~ 7.5 and $\sim 4000 \text{ }\mu\text{S cm}^{-1}$, respectively, which can be categorized in the range of brackish waters.

2.2 Flow-Through Reactor Experiments

A total of seven flow-through reactors (FTRs) were operated to carry out a 3-month experiment. Each FTR was constructed similar to Pallud et al. (2007) by using a Plexiglas tube (those used to collect the soil) connected to polyvinyl chloride (PVC) plate caps with an inlet/outlet opening for tubing connection. Between the soil surface and plate caps on each end of the Plexiglas tube, an O-ring, a $0.45\text{-}\mu\text{m}$ pore size acrylic copolymer disk filter (VWR International) and a $1\text{-}\mu\text{m}$ pore size glass fiber filter (VWR International) were inserted as a flow distributor. A peristaltic pump (Gilson MINIPULSE® 3) was connected to the bottom end-cap of the FTRs and the top end-cap was connected to the effluent sampling vials. PTFE Teflon tubes ($1/8''$ O.D. \times $0.063''$ I.D., Sigma-Aldrich) were employed for inlet and outlet channels, and flow rate was 2.7 mL h^{-1} in the range of

groundwater flow rate at the sampling location during the entire experiment. To simulate underground conditions, FTRs were covered with aluminum foil. A schematic diagram of the column setup is shown in Fig. 1 (a picture of the experimental setup is also attached as Supplementary Material (SM), Figure SM1).

A synthetic influent solution was injected through the FTRs and prepared based on groundwater sample analysis from the site and contained background nutrients including MgCl_2 (89 mg L^{-1}), KCl (24 mg L^{-1}), and $\text{CaCl}_2 \cdot \text{H}_2\text{O}$ (243 mg L^{-1}) in argon-purged Milli-Q water ($\text{DO} < 0.8 \text{ mg L}^{-1}$). Sulfate was supplied during two injection episodes to simulate engineered sulfate injection at the field scale and investigate the effects of a multiple injection scenario (Lebkowska et al. 2011). Since the sulfate mass that can be injected to the sub-surface is limited in practice due to production of inhibitory sulfide (Cunningham et al. 2001), sulfate concentration in the synthetic influent solution was kept at $\sim 150 \text{ mg L}^{-1}$ during both injection episodes. In the first injection episode, naphthalene concentration was $\sim 4 \text{ mg L}^{-1}$ and for the second injection episode, it was increased to $\sim 12 \text{ mg L}^{-1}$. Dissolved sulfate concentration of 150 mg L^{-1} in the synthetic influent solution was significantly higher than the theoretical stoichiometric mass required for the complete mineralization of 4 and

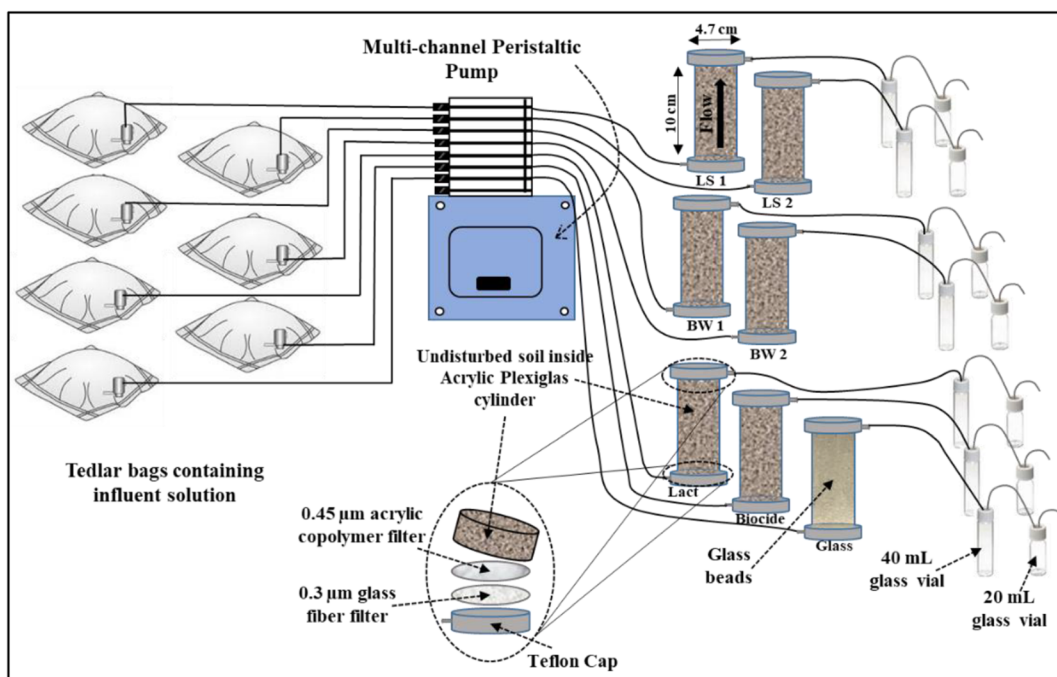


Fig. 1 Schematic diagram of the flow-through reactor (FTR) setup

12 mg L⁻¹ naphthalene during both injection episodes (Galushko et al. 1999). This high sulfate concentration was supplied to ensure SRB development over potentially competing microbes. Although it was expected that even complete degradation of injected naphthalene concentration may not significantly reduce the high sulfate concentration, 150 mg L⁻¹ dissolved sulfate was supplied to provide the most ideal conditions for the development of SRB community. HCl and NaOH solutions were used for the influent solution pH adjustment to be ~ 7. Then, influent solution was transferred to separate 1 L Tedlar bags using a glass syringe under anaerobic conditions. Each Tedlar bag served as a reservoir for each FTR to continuously pump the influent solution into the FTRs (Fig. 1).

The synthetic influent solution containing sulfate, naphthalene, and background nutrients was injected through two FTRs to simulate low salinity (EC = ~ 1000 $\mu\text{S cm}^{-1}$) representing fresh water conditions (identified as LS1 and LS2). To mimic the effects of brackish environments, 1300 mg L⁻¹ NaCl was added to the synthetic influent solution to increase the associated salinity and EC value to the level similar to the sampling location in the brackish coastal environment (4000 $\mu\text{S cm}^{-1}$) and then injected through two FTRs identified as BW1 and BW2. To investigate the soil organic adsorption, one FTR (identified as Biocide)

was also injected similar to the LS FTRs while biocide HgCl₂ (275.5 mg L⁻¹) was also dissolved in the synthetic influent solution to restrict biodegradation process (Van De Graaf et al. 1995). One FTR (identified as Glass) was filled with glass beads (diameter of 3 mm, Sigma-Aldrich) and was injected with the synthetic influent solution containing background nutrients and naphthalene to control the potential naphthalene adsorption to the FTR setup and PTFE tubes. The last FTR (identified as Lact) was injected identical to the LS FTRs, but just naphthalene was replaced by lactate as a preferred carbon source for SRB (Acton and Barker 1992) to control and compare the SRB development. Lactate concentration was kept at ~ 100 mg L⁻¹ during both injection episodes to serve as a control for the re-adaptation of SRB during the second injection episode. Details of the synthetic influent solutions for each FTR are summarized in Table 1.

The experiments ran for 3 months at room temperature (23 ± 2 °C). The influent and effluent solutions were collected regularly to determine naphthalene, anions, and DIC concentrations. In addition, pH, EC, DO, and Eh of the effluent samples were also analyzed. The effluent outlet on top of the FTRs was connected to a 40-mL and a 20-mL glass vials in series to restrict naphthalene volatilization in the collected effluent samples. While both 40- and 20-mL glass vials were always

Table 1 Summary of the FTR specifications and operational conditions

FTRs	Effective			
	Porosity [%]	First injection [PV]	Second injection [PV]	Synthetic influent solution ¹
LS1	37.2	49	35	Nutrients ² , sulfate ³ , naphthalene ⁴
LS2	44.1	37	30	Nutrients ² , sulfate ³ , naphthalene ⁴
BW1	28.5	58	32	Nutrients ² , sulfate ³ , naphthalene ⁴ , NaCl ⁵
BW2	32.4	45	39	Nutrients ² , sulfate ³ , naphthalene ⁴ , NaCl ⁵
Lact	38.9	30	32	Nutrients ² , sulfate ³ , lactate ⁶
Biocide	62.4	22	20	Nutrients ² , sulfate ³ , naphthalene ⁴ , HgCl ₂ ⁷
Glass	48.3	27	20	Nutrients ² , naphthalene ⁴

¹ All the chemicals were dissolved in argon-purged Milli-Q water (DO < 0.8 mg L⁻¹)

² Nutrients include MgCl₂ (89 mg L⁻¹), KCl (24 mg L⁻¹), and CaCl₂·H₂O (243 mg L⁻¹) for all FTRs

³ Sulfate concentration was 150 mg L⁻¹ for all FTRs

⁴ Naphthalene concentration was 4 and 12 mg L⁻¹ during the first and second injection episodes, respectively, for all FTRs

⁵ NaCl concentration in BW FTRs was 1300 mg L⁻¹

⁶ Lactate concentration was 100 mg L⁻¹

⁷ HgCl₂ concentration was 275.5 mg L⁻¹

kept full of aqueous effluent solution, the 40-mL vials which were not in contact with air were always sampled.

The following sequence of steps were applied during the three-month experiment: (1) 3 pore volumes (PVs) of argon-purged Milli-Q water containing background nutrients (with no sulfate or organic compound) were injected to displace pore water and then injection was stopped for 2 weeks to provide anaerobic saturation condition; (2) 5 PVs of argon-purged 100 mg L⁻¹ of NaBr solution containing background nutrients were injected to investigate hydraulic consistency through the analysis of bromide tracer test; (3) FTRs were injected for 35 days by the synthetic influent solution contained 4 mg L⁻¹ naphthalene concentration until the steady-state condition was achieved and then stopped for 1 week under anaerobic saturated condition; (4) to simulate a multiple injection scenario under more intense conditions, the FTRs were again injected for 1 month with 12 mg L⁻¹ naphthalene solution; and (5) when the experimental test was concluded, three soil samples from the inlet (bottom), middle (~5 cm), and outlet (top) of each FTR were collected and analyzed to determine the adsorbed naphthalene concentration.

The Lact FTR was executed to provide the most ideal conditions for SRB development. Although naphthalene degradation within the FTRs could also occur under methanogenic conditions, it is expected that the SRB will outperform methanogens for the available electron donors due to continuous sulfate injection during the experimental period (Dar et al. 2008; Stams et al. 2005; Talbot et al. 2008). Consequently, it was speculated the combination of geochemical indicators such as redox potential, DO, and DIC concentrations along with sulfate consumption within the Lact FTR during 2 months of sulfate injection sufficiently confirm SRB activities within the FTRs, and hence, the results from the Lact FTR could be attributed and compared to other FTRs injected by naphthalene solution. Although a combination of culture-based or genetic-based microbial analyses could better determine the main electron acceptors under the experimental conditions, the collected experimental data set was deemed sufficient for the purpose of this study to investigate the effects of salinity on the engineered sulfate injection as a remediation strategy in the hydrocarbon-contaminated brackish subsurface environments. Methane concentration was not measured during the experimental period due to sulfate injection and development of SRB community which was expected to outperform methanogens.

One of the main objectives of this study was to perform the experiments under dynamic condition to simulate realistic groundwater flow in the subsurface system. While performing the experiments under dynamic flow-through condition may flush a portion of native microbes in the pore water, the microbial community is significantly associated with the soil properties and environmental conditions (Nannipieri et al. 2003). Because soil properties and matrix were not disturbed, the developed microbial community during the experimental period would represent the realistic condition. Additionally, it should be noted that geochemical and microbiological characteristics of the soil and water will change once the contaminants are introduced (ITRC 2011). Hence, it is not expected that the native microbes at the time of sampling perform the biodegradation process but rather, microbial community associated with the new environmental conditions will be developed. For example, sulfate injection enhanced the SRB community in this study that consumed naphthalene as a carbon source. However, the undisturbed soil samples were employed to ensure soil matrix and properties, and also the flow regime and associate developed microbial community can simulate subsurface conditions in the (semi)-arid coastal soil environment.

2.3 Reagents and Analytical Methods

Naphthalene (C₁₀H₈, Sigma-Aldrich), sodium sulfate (Na₂SO₄, Sigma-Aldrich), sodium lactate (C₃H₅NaO₃, Sigma-Aldrich), mercuric chloride (HgCl₂, Sigma-Aldrich), manganese chloride (MgCl₂, Sigma-Aldrich), potassium chloride (KCl, Sigma-Aldrich), calcium chloride (CaCl₂.H₂O, Sigma-Aldrich), sodium chloride (NaCl, Sigma-Aldrich), sodium bromide (NaBr, Sigma-Aldrich), and methylene chloride (CH₂Cl₂, EMD Millipore) were all reagent grade and used as received.

For organic analyses of the aqueous effluent samples similar to Shafieiyoun and Thomson (2018, 2019), 19 mL sample was collected and mixed with 1.0 ml of methylene chloride (containing internal standards metafluoro-toluene and fluoro-biphenyl at 25 mg L⁻¹). The vial was quickly resealed and agitated on its side at 350 rpm on a platform shaker for 20 min. After shaking, the vial was inverted, and the aqueous and organic phases were allowed to separate for 30 min. For the organic analyses of the soil samples at the end of the experiment, 10 mL of methylene chloride was added to 5 g of each soil sample into a 20-mL glass vial which

was quickly resealed and agitated on its side at 175 rpm on a platform shaker for 48 h, after which the vial was left on the bench for 5 days and 17 h for sedimentation of soil particles. For both soil and aqueous samples analyses, approximately 0.7 mL of the methylene chloride phase was removed from the inverted vials with a gas tight glass syringe, through a Teflon septum. The solvent was placed in a Teflon sealed autosampler vial for analysis. All samples were analyzed using a HP 5890 capillary gas chromatograph (GC) connected to a HP7673A autosampler and a flame ionization detector (FID). Three microliters of methylene chloride were injected in splitless mode (purge on 0.5 min, purge off 10 min) onto a 0.25 mm \times 30 m length, DB5 capillary column with a stationary phase film thickness of 0.25 μ m. Helium column flow rate was 2 mL min⁻¹ with a make-up gas flow rate of 30 mL min⁻¹. Injection temperature was 275 °C, detector temperature was 325 °C, and initial column oven temperature was 35 °C held for 0.5 min, then ramped at 15 °C min⁻¹ to a final temperature of 250 °C and held for 2 min. Chromatographic run time was 16 min. Data integration was completed with an SRI Model 302 Peak Simple chromatography data system.

Aqueous effluent samples were filtered through 0.2- μ m pore size polysulfone filters (ThermoFisher Scientific) and analyzed for ion chemistry using a Dionex (Thermo Fisher) ICS-5000 Capillary Ion Chromatograph equipped with an ion eluent generator and conductivity detector. For anions, a 0.4- μ L of sample was injected using a Dionex AS-40 Autosampler onto a Dionex® Ion Pac AS18-RFIC (0.4 \times 250 mm) column. The mobile phase was 26 mM potassium hydroxide (KOH) at a flow rate of 0.01 mL min⁻¹. The chromatograph was obtained using Dionex Chromeleon 7.0 chromatography software®. DIC concentrations of effluent samples were determined using the non-purgeable organic carbon (NPOC) method on a total organic carbon analyzer (Shimadzu TOC-LCPH/CPN). Each sample was analyzed three times and average values were reported along with associated standard deviations. pH, EC, Eh, and DO in the aqueous effluent samples were measured using an Orion™ Versa Star Pro™ portable meter (Thermo Scientific). Eh value was initially measured after removing the cap of 40 mL sampling vial. Enough sample for GC-FID analyses was then collected and pH and EC were measured on those samples. Subsequently, effluent samples for DIC and sulfate concentrations were collected.

3 Results and Discussions

Three PVs of Milli-Q water were injected at the beginning of the experiments to displace the pore water in the soil matrix, provide saturated condition, and develop a new steady condition in the soil under anaerobic condition which is the most dominant mechanism in the organic contaminated subsurface systems. Following development of anaerobic condition, tracer test and actual experiments were initiated. Breakthrough curves of the measured Br⁻ concentration in the effluent pore waters are illustrated in Figure SM2. For all the FTRs, after \sim 1 PV, the Br⁻ concentration reached to \sim 50% of the initial concentration, and after \sim 2 PVs reached to 100% (\sim 100 mg L⁻¹). The effective porosity was calculated using the breakthrough curve analysis (Weber and DiGiano 1995). A summary of the effective porosities and operational conditions of the FTRs is listed in Table 1. Since undisturbed soil was used for the purpose of these experiments, the effective porosity differed between FTRs, and hence, the total PVs injected during the experimental period were different (Table 1).

No significant difference was observed between the influent and effluent EC values in all FTRs and the values were \sim 1000 and 4000 μ S cm⁻¹ for the LS and BW FTRs, respectively. Effluent dissolved sulfate and nitrate concentrations resulted from the soil content for all the FTRs was initially \sim 140 and 8 mg L⁻¹, respectively, but after injecting \sim 5 PVs of solution during the Br⁻ tracer tests, they decreased to less than the method detection limit (MDL) of 0.5 mg L⁻¹. The effluent pH for the Glass FTR was the same in the influent solution, but for the other FTRs increased from \sim 7 in the input solutions to \sim 8 while the BW FTRs had the highest effluent pH. The increase of the effluent pH can be attributed to the soil alkalinity as well as the sulfate reduction and production of weaker acids. While no physical changes were observed in the Glass and Bio-cide FTRs, the soil color in the Lact FTR became darker (black) after 2 weeks of injection. The black color was initially generated in the second half and near the top outlet of the Lact FTR and then distributed within the entire FTR column (see Figure SM3). This change in soil color can serve as an indicator for the SRB growth and attributed to the black iron sulfide precipitates generated due to the reaction of iron from the soil content with hydrogen sulfide produced during the sulfate reduction (Acton and Barker 1992). The color of the soils in the LS and BW FTRs also became darker after

1 month of injection. The change in FTRs was coincident with reduction in the Eh profiles.

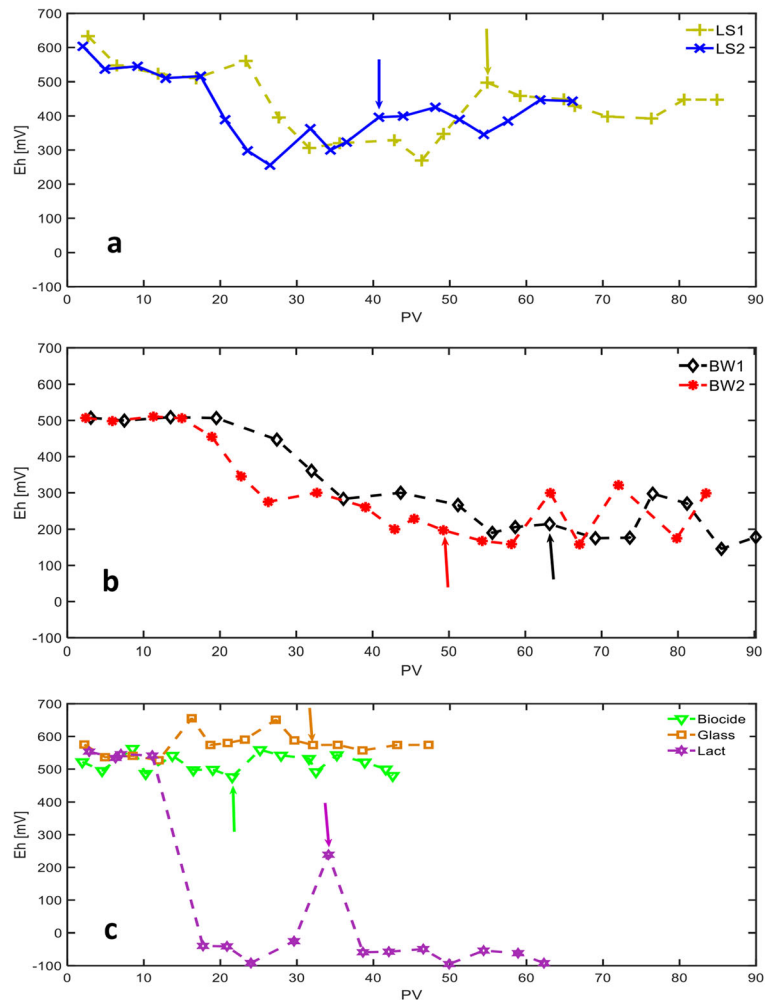
3.1 Development of Reducing Conditions

Effluent Eh values of the FTRs are shown in Fig. 2. The optimal oxidation-reduction potential (ORP) for the sulfate reduction is -200 mV (Eh of ~ 0 mV at 20 °C) (Cassidy et al. 2015) and Eh results can serve as an indicator for any shift toward the reducing conditions. Eh values in the influent solutions were $> +500$ mV and did not change in the effluent of the Biocide and Glass FTRs, indicating that microbial activities were successfully restricted (Fig. 2c). As expected, the redox potential initially dropped in the Lact FTR from 550 to -40 mV after ~ 15 PVs (i.e., 2 weeks), indicating the enhancement of reducing conditions and enhancement

of anaerobic biodegradation (Fig. 2c). Following the initial rapid drop, the effluent Eh from the Lact FTR gradually decreased to -90 mV after 25 PVs followed by minor fluctuations until the end of the experiments. The peak at 34 PVs is related to the 4th PV following the beginning of the second injection episode. However, the redox potential again dropped to -60 mV after 39 PVs indicating the re-adaptation of microbial community and specifically SRB during the second injection episode. Previous studies also confirmed that the SRB have high potential for re-adaptation against the environmental stresses (e.g. Dolla et al. 2006).

The effluent Eh from the LS and BW FTRs dropped after 20 to 25 PVs. In the LS FTRs, the initial drop was followed by fluctuations around $+300$ mV until the end of the first injection episode. Following the second injection, the effluent Eh for the LS FTRs increased to

Fig. 2 Effluent Eh values from (a) low salinity (LS1 and LS2) FTRs, (b) brackish water (BW1 and BW2) FTRs, and (c) Biocide, Glass, and Lact FTRs. Each arrow represents the first sampling following the beginning of the second injection episode. Due to differences in the effective porosity of the undisturbed soil sample in each FTR, the number of injected PVs in each FTR and also place of the arrows are not the same



~400 mV by the end of the experiments. The behavior of the effluent Eh in the BW FTRs was (1) after 20–25 PVs initially dropped to ~300 mV and then decreased to <200 mV by the end of the first injection episode, (2) following the second injection, the effluent Eh initially remained stable for ~10 PVs in the range of 100 to 200 mV, (3) after ~15 PVs following the second injection episode and introducing the higher naphthalene concentration, the effluent Eh values increased and fluctuated in the range of 200 to 300 mV.

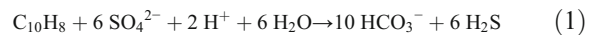
Overall, the data from the redox potential in the FTRs indicate a notable decrease in the Eh values and the reducing conditions within the FTRs followed the order: Lact > BW > LS > Biocide \cong Glass. The comparison of the results between the LS and BW FTRs indicates that stronger and more persistent reducing conditions were developed inside the BW FTRs which were injected by higher salinity solution similar to the brackish condition in the (semi)-arid coastal area. Following the second injection episode, in the Lact FTR, which was fed by a constant concentration of a more preferred carbon source, the effluent Eh was initially increased indicating that SRB activity was inhibited probably due to lack of sufficient sulfate and carbon source. However, SRB again readapted and effluent Eh returned to the levels similar to the first injection episode. For the LS and BW FTRs, which were injected with a higher naphthalene concentration following the second injection episode, the effluent Eh increased compared to the first injection episode but the BW FTRs were more stable against the stresses resulted by changes in naphthalene concentration.

It should be noted that the mismatch of the initial drops between the Eh profiles of the LS1 and LS2 FTRs (Fig. 2a) can be attributed to their different effective porosities. While the flow rates were similar in both LS1 and LS2 FTRs, the higher porosity of the LS2 FTR resulted in a larger PV and hence, a fewer PVs would be required to supply the same sulfate mass compared to the LS1 FTR. The same trend was also observed between the BW FTRs.

3.2 Sulfate Reduction

Various degradation pathways for the complete mineralization (Lovley et al. 1995) or partial degradation (Abbasian et al. 2015; Grbic-Galic and Vogel 1987; Meckenstock et al. 2016) of some organic compounds under anaerobic condition have been suggested. During complete mineralization of naphthalene and lactate under sulfate-reducing

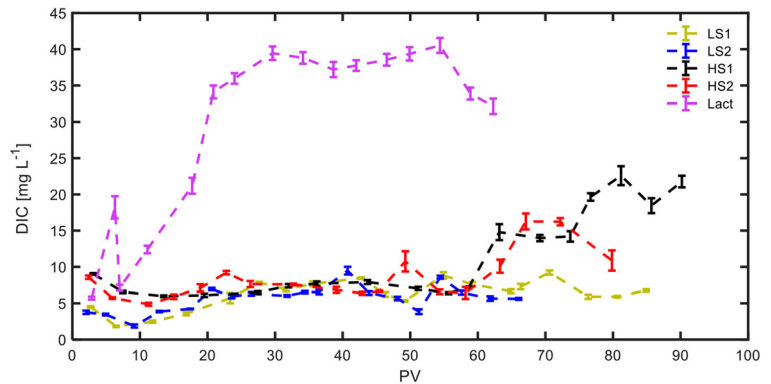
condition, DIC is generated according to the following reactions (El Bayoumy et al. 1999; Galushko et al. 1999):



In this study, the effluent DIC concentrations as an indicator for the naphthalene mineralization were measured and presented in Fig. 3. As expected, the Lact FTR had the highest DIC effluent concentrations and the DIC from the BW FTRs were slightly higher than those from the LS FTRs, especially at the end of the second injection episode, suggesting that naphthalene degradation was more enhanced in the BW FTRs that led to complete mineralization through the degradation pathways. For all BW and LS FTRs, DIC concentrations initially dropped probably due to depletion of the soil inorganic carbon content but increased gradually after ~20 PVs until the end of the experiments. The increase in DIC concentration is coincident with reducing condition enhancement (Fig. 2) and can be attributed to the complete mineralization of naphthalene. The BW1 FTR had the highest DIC effluent concentration after the Lact FTR.

The ratios of the effluent sulfate concentrations to initial injected concentrations are shown in Fig. 4. The Lact FTR showed the highest sulfate reduction that decreased to ~15% of the injected concentration. At the beginning of the second injection episode, effluent sulfate concentration from the Lact FTR sharply increased to 80% that is coincident with the peak at the 34th PV in the Eh profile (see Fig. 2c), indicating that sulfate reduction is due to development of reducing conditions and SRB activities. As expected, the effluent sulfate concentration for the LS and BW FTRs did not decrease significantly because the injected sulfate concentration was very high compared to the injected dissolved naphthalene concentration. However, 150 mg L⁻¹ sulfate concentration was supplied to provide the most ideal condition for the enhancement of SRB community and ensure SRB development over potentially competing microbes such as methanogens (Dar et al. 2008; Stams et al. 2005; Talbot et al. 2008). In a complex environment such as soil, a wide range of degradation pathways can occur and it is not possible to determine the exact stoichiometric ratios (Meckenstock et al. 2016). However, based on Reaction 1 for the

Fig. 3 Effluent dissolved inorganic carbon (DIC) concentrations from the FTRs. The error bars represent the standard deviation from three measurements



complete mineralization of naphthalene under sulfate-reducing condition, the sulfate concentration was ~ 8 times more than the theoretical mass required to completely degrade the injected naphthalene. Hence, the effluent sulfate consumption was not expected to reach $< 85\%$ even if the total naphthalene mass could be degraded due to sulfate reduction. For all the LS and BW FTRs, the effluent sulfate concentrations fluctuated between 90 and 97% of the injected concentration and a minor decrease was observed following the second injection episode for the BW FTRs.

Overall, the general trends of the geochemical indicators were similar between the Lact, LS, and BW FTRs. The notable decrease of the redox potential in the effluent of the LS, BW, and Lact FTRs, as well as the sulfate reduction, black color in the soil, and DIC generation, indicates the reducing conditions enhancement and SRB activity following sulfate injection.

3.3 Naphthalene Degradation

The ratios of the effluent naphthalene concentrations to influent injected concentrations are presented in Fig. 5. The effluent concentration from the Glass FTR initially

increased gradually from ~ 70 to $\sim 85\%$ by the end of the first injection episode. Following the second injection episode and introducing higher naphthalene concentration, the effluent concentration initially dropped to 46% of the injected concentration due to changes in the equilibrium sorbed concentration. By the end of the second injection episode, effluent naphthalene concentration reached to $\sim 85\%$ indicating despite all attempts to use resistant materials against the abiotic loss of organic compounds, $\sim 15\%$ of the injected naphthalene was adsorbed by the FTR setups and Teflon tubes or evaporated during sampling. The effluent naphthalene concentration from the Biocide FTR was initially $\sim 20\%$, but due to saturation of the soil adsorption capacity, gradually increased to $\sim 85\%$ (similar to the Glass FTR) by the end of the first injection episode (22 PVs). Following the second injection episode, the naphthalene effluent concentration decreased to $\sim 58\%$, but eventually reached to 85% by the end of the experiments.

For the LS and BW FTRs, the initial naphthalene effluent concentration was $< 5\%$ of the injected concentration (Fig. 5). The comparison of naphthalene mass balance analyses between the Biocide FTR with LS and

Fig. 4 Ratio of effluent sulfate concentrations to the injected sulfate concentrations from the FTRs. Injected sulfate concentration was 150 mg L⁻¹

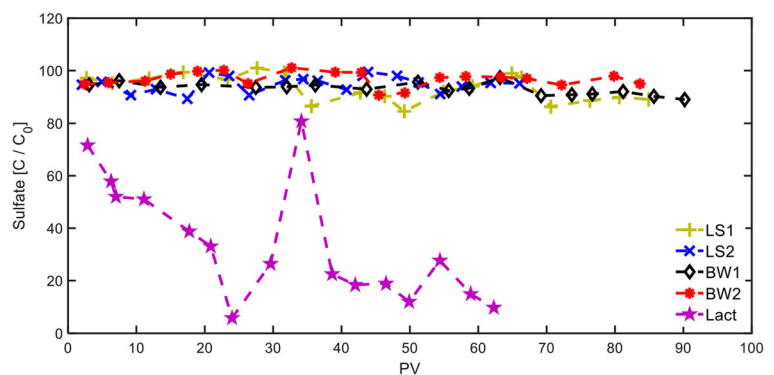
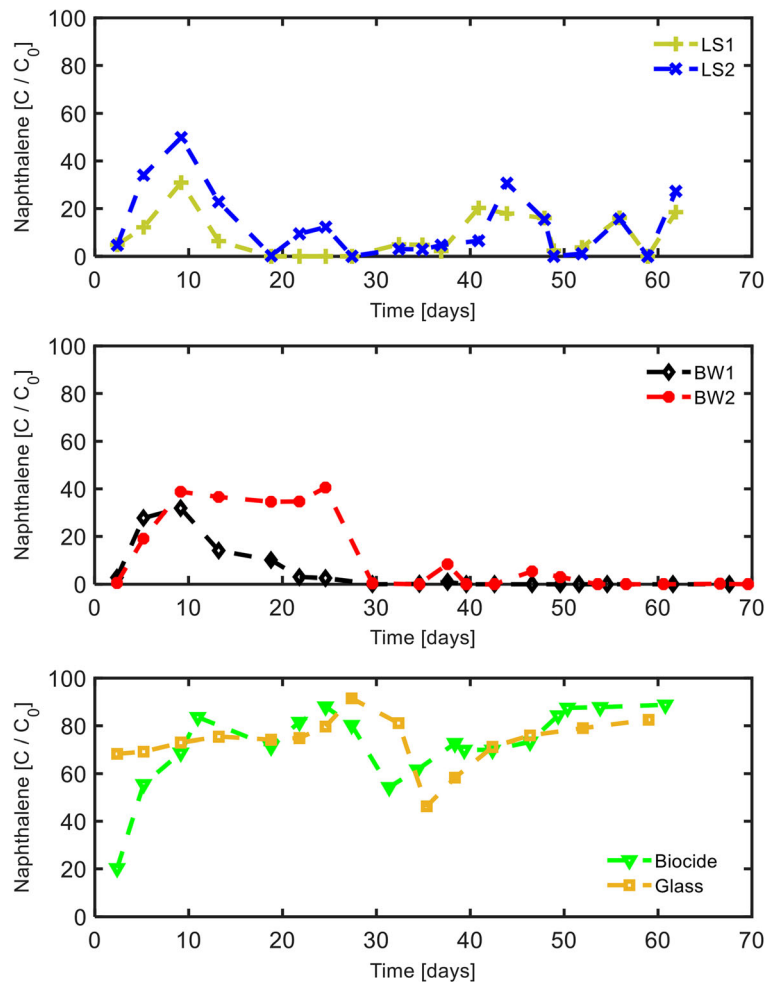


Fig. 5 Ratio of naphthalene effluent concentration to initial injected concentration from the (a) low salinity (LS1 and LS2) FTRs, (b) brackish water (BW1 and BW2) FTRs, and (c) Biocide and Glass FTRs. Injected naphthalene concentration was 4 and 12 mg L⁻¹ during the first and second injection episodes, respectively



BW FTRs indicates that at the beginning of the injection only ~15% of the injected mass was degraded and ~80% was adsorbed. The naphthalene effluent concentrations from the LS and BW FTRs initially increased until ~10 days and reached to a maximum concentration. This initial increase was caused because the soil adsorption capacity gradually saturated while reducing conditions and SRB were still not developed (see Fig. 2). The FTRs with higher effective porosities (LS2 and BW2) indicated higher maximum naphthalene effluent concentrations which can be attributed to their lower soil mass as well as less contact of naphthalene with the soil particles and hence, less potential for the soil adsorption.

For the LS FTRs, the naphthalene effluent concentrations dropped after ~10 days and reached to the MDL by the end of the first injection episode (35 days or 49 PVs for LS1 and 37 PVs for LS2). The decrease in the naphthalene concentration after 10 days can be

attributed to the enhancement of anaerobic biodegradation which was also reflected in effluent Eh and sulfate concentration (Figs. 2 and 4). Naphthalene mass balance calculations for the LS FTRs indicate that at the end of the first injection episode, ~15% of the mass loss was due to adsorption and ~80% by biodegradation. To investigate the effectiveness of biodegradation under more contaminated conditions, naphthalene influent concentration was increased during the second injection episode. While the soil adsorption increased following the second injection episode (based on the results from the Biocide FTR), the naphthalene effluent concentrations also increased in the LS FTRs and reached to ~20% of the injected concentration.

The behavior of the BW FTRs was similar to the LS FTRs during the first injection episode. Naphthalene effluent concentration initially increased from <5% of the injected concentrations to ~30–40% after ~10 days

and then gradually decreased to ~MDL by the end of the first injection episode (35 days). Following the second injection episode, the effluent naphthalene concentrations from the BW FTRs remained stable and were not affected. In summary, both LS and BW FTRs showed similar behavior during the first injection episode. Following the second injection episode and introducing a higher naphthalene concentration, the effluent concentration from the BW FTRs was still <MDL, while for the LS FTRs increased. The dynamic nature of the effluent naphthalene concentration during the second injection episode was also reflected in the increase of the effluent Eh (Fig. 2) which was more significant for the LS FTRs. Effluent Eh values of the LS FTRs reached to more than 400 mV during the second injection episode suggesting that the biodegradation was inhibited by increasing the naphthalene concentration.

The combination of geochemical indicators and effluent naphthalene concentrations in this study indicated that while increasing the injected naphthalene concentration did not affect biodegradation efficiency for the BW FTRs, adversely restricted the developed reducing conditions and microbial activities for the LS FTRs. Hence, biodegradation efficiency was limited for the LS FTRs and effluent naphthalene concentration fluctuated in the range of <MDL to ~20% of the injected concentration. It can be hypothesized that the higher naphthalene concentration during the second injection episode affected the system like the biocide substance and resulted in substrate toxicity (Abuhamed et al. 2004) specifically for the LS conditions. As opposed to the substantial body of previous studies that salinity restricts biodegradation (Abed et al. 2015; Ajisebutu 1988; Brusa et al. 2001; María Piedad Díaz et al. 2000; Mille et al. 1991; Thamer et al. 2013; Ward and Brock 1978), the results from this study indicated that naphthalene biodegradation was more enhanced in the BW FTRs compared to the LS FTRs probably because microbial cultures within the undisturbed soil were adapted to the brackish water conditions at the field sampling environment. The increase in naphthalene concentration may cause a rearrangement of microbes involved in biodegradation process and probably microbes thriving in a less salted environment are more susceptible to the increase in naphthalene concentration compared to the salt adapted microbes. Consequently, while increasing the injected naphthalene concentration did not affect the effluent naphthalene concentration of the BW FTRs, resulted in dynamic and fluctuating unsteady effluent concentrations for the LS FTRs.

The sorbed naphthalene concentrations at the inlet, middle, and outlet of each FTR were determined at the end of the experimental period. Since all FTRs were injected by constant 12 mg L⁻¹ naphthalene solution over the second injection episode of the experiments for 1 month, the final naphthalene concentrations in soil were considered as equilibrium sorbed concentrations. While the sorbed naphthalene concentrations at the end of the experimental period near the inlet were in the range of 1.1 to 2.5 mg kg⁻¹ with no clear trend, the sorbed concentrations near the outlet, at the top of the FTRs, were < 50% of those near the inlet for each FTR and followed the order of BW < LS < Biocide. This is confirming that the BW FTRs had lower effluent aqueous naphthalene concentrations compared to the LS FTRs. For the Biocide FTR, the sorbed concentration was relatively unchanged throughout the FTR, suggesting that naphthalene aqueous concentration did not change along the pathway. For the BW and LS FTRs, sorbed naphthalene concentrations did not decrease significantly in the first half of the FTRs, suggesting that sulfate reduction and biodegradation dominated at the second half of the FTRs. This change agrees with the distribution of black color (Figure SM3) that was also initially observed in the upper part of the FTRs. In addition, this condition is similar to the column experiments investigated by Sinke et al. (1998), where the sulfate reduction was dominated in the second half of the column after 15 weeks of injection. This can be attributed to more aggressive anaerobic condition over the second half of the FTRs that enhanced naphthalene degradation, while in the first half of the FTRs, the sorbed concentration and probably dissolved phase did not change significantly. For the BW1 FTR, the sorbed naphthalene concentration at the outlet was <MDL. This can be attributed to more enhanced biodegradation in the BW1 FTR that was also reflected in the Eh and effluent naphthalene profiles where the most notable dissolved naphthalene degradation and associated reducing conditions were occurred in the BW1 FTR. After 30 days (40 PVs) injection, naphthalene was no longer detected in the effluent of the BW1 FTR (Fig. 5), and hence, the sorbed naphthalene concentration was below the MDL at the outlet.

The results from the Biocide FTR indicate that 33% of the injected naphthalene mass was adsorbed. Mass balance calculations for the LS1 and LS2 FTRs indicated that 85 and 80% of the injected naphthalene mass was consumed, respectively and when compared to the

results from the Biocide FTR, approximately 50% of the injected naphthalene mass was degraded. Similarly, for the BW FTRs, ~60% of the injected naphthalene mass was degraded. The overall stoichiometry for these FTR systems can be estimated as the ratio of sulfate reduced to naphthalene mass degraded. The average estimates of overall stoichiometry (corrected for adsorption) were 2.3 for the LS FTRs and 1.95 for the BW FTRs. These data provide insight into the ability of the investigated systems to degrade dissolved naphthalene in the contaminated groundwater under sulfate-reducing conditions. The theoretical stoichiometry mass ratio for the naphthalene degradation under sulfate-reducing condition (see Reaction 1) is 4.5 g-sulfate/g of the naphthalene which is ~2 times more than the stoichiometry ratios estimated in this study. This difference can be attributed to the wide range of degradation pathways (Meckenstock et al. 2016) which can be applied by different bacterial strains in the soil as well as various side reactions which can enhance or inhibit the biodegradation process.

4 Summary and Conclusion

The aim of this study was to identify the effects of salinity on the performance of sulfate injection in a system representing the in situ groundwater anaerobic conditions. It was intended to assemble an informative data set including geochemical indicators (i.e., Eh, pH, EC, DO, DIC), soil porosity, soil adsorption, and dissolved phase concentrations to identify hydrocarbon-contaminated subsurface responses to engineered sulfate application at different salinity conditions.

The results indicated that combination of all the geochemical adsorption data along with dissolved organic concentrations can provide an improved understanding of the hydrocarbon-contaminated subsurface responses to the engineered sulfate injection. The sulfate reduction, black color in the soil, DIC generation, and the notable decrease of the redox potential in the effluent of the FTRs, which were injected with synthetic contaminated groundwater containing dissolved naphthalene, indicated the reducing conditions development and SRB activities. As expected, reducing conditions in the FTRs injected by naphthalene solution were less enhanced by sulfate application compared to the one injected by lactate; however, the general trends of the geochemical indicators were similar between them. As opposed to the substantial body of previous

studies that salinity restricts biodegradation, the results indicated that engineered sulfate injection for the dissolved naphthalene degradation in the undisturbed soil samples collected from the (semi)-arid brackish coastal soil was more stable under brackish water conditions similar to the field condition in this study. This highlights the adaptation of the microbial communities within the undisturbed soil to the higher salinity conditions at the brackish coastal soil environment suggesting microbes thriving in a less salted environment are more susceptible to the increase in naphthalene concentration compared to the salt adapted microbes. The results of this study provide insight into anaerobic bioremediation of the hydrocarbon-contaminated brackish environments and indicate that not only dissolved phase degradation is not limited by salinity in the brackish environments, but also it is more enhanced and stable against the environmental stresses. It is suggesting that the salinity of the injected solution during the design and implementation of the engineering sulfate application in the brackish coastal environments should be adjusted to be in the range of groundwater conditions.

Acknowledgments The findings achieved herein are solely the responsibility of the authors. We also would like to acknowledge the funding provided by the Canada Excellence Research Chair program in Ecohydrology. We are thankful to Marianne Vandergriendt, Shirley Chatten, Lindsay Norwood, and Jamal Hannun for their valuable assistance during the experiments and sample analyses.

Funding Information Open Access funding provided by the Qatar National Library. This study was funded by NPRP grant # NPRP9-93-1-021 from the Qatar national research fund (a member of Qatar Foundation).

Compliance with Ethical Standards

Conflict of Interest The authors declare that they have no conflict of interest.

Open Access This article is licensed under a Creative Commons Attribution 4.0 International License, which permits use, sharing, adaptation, distribution and reproduction in any medium or format, as long as you give appropriate credit to the original author(s) and the source, provide a link to the Creative Commons licence, and indicate if changes were made. The images or other third party material in this article are included in the article's Creative Commons licence, unless indicated otherwise in a credit line to the material. If material is not included in the article's Creative Commons licence and your intended use is not permitted by statutory regulation or exceeds the permitted use, you will need to obtain permission directly from the copyright holder. To view a copy of this licence, visit <http://creativecommons.org/licenses/by/4.0/>.

References

- Abbasian, F., Lockington, R., Mallavarapu, M., & Naidu, R. (2015). A comprehensive review of aliphatic hydrocarbon biodegradation by bacteria. *Applied Biochemistry and Biotechnology*, 176, 670–699. <https://doi.org/10.1007/s12010-015-1603-5>.
- Abed, R. M. M., Al-kharusi, S., & Al-hinai, M. (2015). Effect of biostimulation, temperature and salinity on respiration activities and bacterial community composition in an oil polluted desert soil. *Int. Biodeterior. Biodegradation*, 98, 43–52. <https://doi.org/10.1016/j.ibiod.2014.11.018>.
- Abuhamed, T., Bayraktar, E., Mehmetoğlu, T., & Mehmetoğlu, Ü. (2004). Kinetics model for growth of *Pseudomonas putida* F1 during benzene, toluene and phenol biodegradation. *Process Biochemistry*, 39, 983–988. [https://doi.org/10.1016/S0032-9592\(03\)00210-3](https://doi.org/10.1016/S0032-9592(03)00210-3).
- Acton, D. W., & Barker, J. F. (1992). In situ biodegradation potential of aromatic hydrocarbons in anaerobic groundwaters. *Journal of Contaminant Hydrology*, 9, 325–352. [https://doi.org/10.1016/0169-7722\(92\)90002-V](https://doi.org/10.1016/0169-7722(92)90002-V).
- Ajisebutu, S. O. (1988). Effects of sodium chloride on biodegradation of crude oils by two species of *Aeromonas*. *Applied Microbiology and Biotechnology*, 28, 203–208.
- Al-Raoush, R. I. (2014). Experimental investigation of the influence of grain geometry on residual NAPL using synchrotron microtomography. *Journal of Contaminant Hydrology*, 159, 1–10. <https://doi.org/10.1016/j.jconhyd.2014.01.008>.
- Anderson, R. T., & Lovley, D. R. (1997). Ecology and biogeochemistry of in situ groundwater bioremediation. In J. G. Jones (Ed.), *Advances in Microbial Ecology*.
- Ben-Dov, E., Kushmaro, A., & Brenner, A. (2009). Long-term surveillance of sulfate-reducing bacteria in highly saline industrial wastewater evaporation ponds. *Saline Systems*, 5, 1–5. <https://doi.org/10.1186/1746-1448-5-2>.
- Bento, F. M., Camargo, F. A. O., Okeke, B. C., & Frankenberger, W. T. (2005). Comparative bioremediation of soils contaminated with diesel oil by natural attenuation, biostimulation and bioaugmentation. *Bioresource Technology*, 96, 1049–1055. <https://doi.org/10.1016/j.biortech.2004.09.008>.
- Birak, P. S., & Miller, C. T. (2009). Dense non-aqueous phase liquids at former manufactured gas plants: challenges to modeling and remediation. *Journal of Contaminant Hydrology*, 105, 81–98. <https://doi.org/10.1016/j.jconhyd.2008.12.001>.
- Boll, M., Fuchs, G., & Heider, J. (2002). Anaerobic oxidation of aromatic compounds and hydrocarbons. *Chemistry & Biology*, 49, 604–611.
- Brusa, T., Borin, S., Ferrari, F., Sorlini, C., Corselli, C., & Daffonchio, D. (2001). Aromatic hydrocarbon degradation patterns and catechol 2, 3-dioxygenase genes in microbial cultures from deep anoxic hypersaline lakes in the eastern Mediterranean sea. *Microbiological Research*, 156, 49–57.
- Burland, S. M., & Edwards, E. A. (1999). Anaerobic benzene biodegradation linked to nitrate reduction. *Applied and Environmental Microbiology*, 65, 529–533.
- Capone, D. G., & Kiene, R. P. (1988). Comparison of microbial dynamics in marine and freshwater sediments. *Limnology and Oceanography*, 33, 725–749.
- Cassidy, D. P., Srivastava, V. J., Dombrowski, F. J., & Lingle, J. W. (2015). Combining in-situ chemical oxidation, stabilization and anaerobic bioremediation in a single application to reduce contaminant mass and leachability in soil. *Journal of Hazardous Materials*, 297, 347–355. <https://doi.org/10.1016/j.jhazmat.2015.05.030>.
- Caumette, P. (1986). Phototrophic sulfur bacteria and sulfate-reducing bacteria causing red waters in a shallow brackish coastal lagoon (Prévost Lagoon, France). *FEMS Microbiology Letters*, 38, 113–124. [https://doi.org/10.1016/0378-1097\(86\)90148-5](https://doi.org/10.1016/0378-1097(86)90148-5).
- Coates, J. D., Anderson, R. T., Woodward, J. C., Phillips, E. J. P., & Lovley, D. R. (1996). Anaerobic hydrocarbon degradation in petroleum-contaminated harbor sediments under sulfate-reducing and artificially imposed iron-reducing conditions. *Environmental Science & Technology*, 30, 2784–2789. <https://doi.org/10.1021/es9600441>.
- Cunningham, J. A., Rahme, H., Hopkins, G. D., Lebron, C., & Reinhard, M. (2001). Enhanced in situ bioremediation of BTEX-contaminated groundwater by combined injection of nitrate and sulfate. *Environmental Science & Technology*, 35, 1663–1670. <https://doi.org/10.1021/es001722t>.
- Dar, S. A., Kleerebezem, R., Stams, A. J. M., Kuenen, J. G., & Muyzer, G. (2008). Competition and coexistence of sulfate-reducing bacteria, acetogens and methanogens in a lab-scale anaerobic bioreactor as affected by changing substrate to sulfate ratio. *Applied Microbiology and Biotechnology*, 78, 1045–1055. <https://doi.org/10.1007/s00253-008-1391-8>.
- Davis, G. B., Barber, C., Power, T. R., Thierrin, J., Patterson, B. M., Rayner, J. L., & Wu, Q. (1999). The variability and intrinsic remediation of a BTEX plume in anaerobic sulphate-rich groundwater. *Journal of Contaminant Hydrology*, 36, 265–290. [https://doi.org/10.1016/S0169-7722\(98\)00148-X](https://doi.org/10.1016/S0169-7722(98)00148-X).
- Díaz, M. P., Grigson, S. J. W., Peppiatt, C. J., & Burgess, J. G. (2000). Published studies in this area have been mostly focused on the organisms and mechanisms in which different organic compounds can be degraded. *Marine Biotechnology*, 2, 522–532.
- Dolla, A., Fournier, M., & Dermoun, Z. (2006). Oxygen defense in sulfate-reducing bacteria. *Journal of Biotechnology*, 126, 87–100. <https://doi.org/10.1016/j.jbiotec.2006.03.041>.
- El Bayoumy, M. A., Bewtra, J. K., Ali, H. I., & Biswas, N. (1999). Sulfide production by sulfate reducing bacteria with lactate as feed in an upflow anaerobic fixed film reactor. *Water, Air, and Soil Pollution*, 112, 67–84. <https://doi.org/10.1023/A:1005016406707>.
- Foti, M., Sorokin, D. Y., Lomans, B., Mussman, M., Zacharova, E. E., Pimenov, N. V., Kuenen, J. G., & Muyzer, G. (2007). Diversity, activity, and abundance of sulfate-reducing bacteria in saline and hypersaline soda lakes. *Applied and Environmental Microbiology*, 73, 2093–2100. <https://doi.org/10.1128/AEM.02622-06>.
- Fuchs, G., Boll, M., & Heider, J. (2011). Microbial degradation of aromatic compounds—from one strategy to four. *Nature Reviews. Microbiology*, 9, 803–816. <https://doi.org/10.1038/nrmicro2652>.
- Galushko, A., Minz, D., Schink, B., & Widdel, F. (1999). Anaerobic degradation of naphthalene by a pure culture of a novel type of marine sulphate-reducing bacterium.

- Environmental Microbiology*, 1, 415–420. <https://doi.org/10.1046/j.1462-2920.1999.00051.x>.
- Gan, S., Lau, E. V., & Ng, H. K. (2009). Remediation of soils contaminated with polycyclic aromatic hydrocarbons (PAHs). *Journal of Hazardous Materials*, 172, 532–549. <https://doi.org/10.1016/j.jhazmat.2009.07.118>.
- García-Blanco, S., Suidan, M.T., Huang, T., Cacho-Rivero, J., Venosa, A.D., 2001. Microcosm study of effect of different nutrient addition on bioremediation of fuel oil no. 2 in soil from Nova Scotia coastal marshes, in: International Oil Spill Conference Proceedings. pp. 309–314.
- Godlefs, A., Tawari, F., Eruke, O., & Ehinomen, I. (2015). Bioremediation, biostimulation and bioaugmentation: a review. *International Journal of Environmental Bioremediation*, 3, 28–39. <https://doi.org/10.12691/ijebb-3-1-5>.
- Grbic-Galic, D., & Vogel, T. M. (1987). Transformation of toluene and benzene by mixed methanogenic cultures. *Applied and Environmental Microbiology*, 53, 254–260.
- Henry, B. M. (2010). Biostimulation for anaerobic bioremediation of chlorinated solvents. In H. Stroo & C. Ward (Eds.), *In situ remediation of chlorinated solvent plumes. SERDP/ESTCP environmental remediation technology*. New York: Springer. https://doi.org/10.1007/978-1-4419-1401-9_12.
- Jain, P. K., Gupta, V. K., Gaur, R. K., Lowry, D. P., Jaroli, D. P., & Chauhan, U. K. (2011). Bioremediation of petroleum oil contaminated soil and water. *Research Journal of Environmental Toxicology*, 5, 1–26. <https://doi.org/10.3923/rjet.2011.1.26>.
- Kauppi, S., Sinkkonen, A., & Romantschuk, M. (2011). Enhancing bioremediation of diesel-fuel-contaminated soil in a boreal climate: comparison of biostimulation and bioaugmentation. *International Biodeterioration & Biodegradation*, 65, 359–368. <https://doi.org/10.1016/j.ibiod.2010.10.011>.
- Laanbroek, H. J., & Pfennig, N. (1981). Oxidation of short-chain fatty acids by sulfate-reducing bacteria in freshwater and in marine sediments. *Archives of Microbiology*, 128, 330–335. <https://doi.org/10.1007/BF00422504>.
- Lebkowska, M., Zborowska, E., Karwowska, E., Miałkiewicz-Peska, E., Muszyński, A., Tabernačka, A., Naumczyk, J., & Jeczalik, M. (2011). Bioremediation of soil polluted with fuels by sequential multiple injection of native microorganisms: field-scale processes in Poland. *Ecological Engineering*, 37, 1895–1900. <https://doi.org/10.1016/j.ecoleng.2011.06.047>.
- Lovley, D. R., & Lonergan, D. J. (1990). Anaerobic oxidation of toluene, phenol, and para-cresol by the dissimilatory iron-reducing organism, GS-15. *Applied and Environmental Microbiology*, 56, 1858–1864.
- Lovley, D. R., Baedeker, M. J., Lonergan, D. J., Cozzarelli, I. M., Phillips, E. J. P., & Siegel, D. I. (1989). Oxidation of aromatic contaminants coupled to microbial iron reduction. *Nature*, 339(6222), 297–300.
- Lovley, D. R., Coates, J. D., Woodward, J. C., & Phillips, E. J. P. (1995). Benzene oxidation coupled to sulfate reduction. *Applied and Environmental Microbiology*, 61, 953–958.
- Meckenstock, R. U., Boll, M., Mouttaki, H., Koelschbach, J. S., Cunha Tarouco, P., Weyrauch, P., Dong, X., & Himmelberg, A. M. (2016). Anaerobic degradation of benzene and polycyclic aromatic hydrocarbons. *Journal of Molecular Microbiology and Biotechnology*, 26, 92–118. <https://doi.org/10.1159/000441358>.
- Megharaj, M., Ramakrishnan, B., Venkateswarlu, K., Sethunathan, N., & Naidu, R. (2011). Bioremediation approaches for organic pollutants: a critical perspective. *Environment International*, 37, 1362–1375. <https://doi.org/10.1016/j.envint.2011.06.003>.
- Mercer, J. W., & Cohen, R. M. (1990). A review of immiscible fluids in the subsurface: properties, models, characterization and remediation. *Journal of Contaminant Hydrology*, 6, 107–163.
- Miao, Z., Brusseau, M. L., Carroll, K. C., Carreón-Diazconti, C., & Johnson, B. (2012). Sulfate reduction in groundwater: characterization and applications for remediation. *Environmental Geochemistry and Health*, 34, 539–550. <https://doi.org/10.1007/s10653-011-9423-1>.
- Mille, G., Almallah, M., Bianchi, M., Van Wambeke, F., & Bertrand, J. C. (1991). Effect of salinity on petroleum biodegradation. *Fresenius' Journal of Analytical Chemistry*, 339, 788–791.
- Müller, J. B., Ramos, D. T., Larose, C., Fernandes, M., Lazzarin, H. S. C., Vogel, T. M., & Corseuil, H. X. (2017). Combined iron and sulfate reduction biostimulation as a novel approach to enhance BTEX and PAH source-zone biodegradation in biodiesel blend-contaminated groundwater. *Journal of Hazardous Materials*, 326, 229–236. <https://doi.org/10.1016/j.jhazmat.2016.12.005>.
- Musat, F., Galushko, A., Jacob, J., Widdel, F., Kube, M., Reinhardt, R., Wilkes, H., Schink, B., & Rabus, R. (2009). Anaerobic degradation of naphthalene and 2-methylnaphthalene by strains of marine sulfate-reducing bacteria. *Environmental Microbiology*, 11, 209–219. <https://doi.org/10.1111/j.1462-2920.2008.01756.x>.
- Nannipieri, P., Ascher, J., Ceccherini, M. T., Landi, L., Pietramellara, G., & Renella, G. (2003). Microbial diversity and soil functions. *European Journal of Soil Science*, 54, 655–670. <https://doi.org/10.1046/j.1351-0754.2003.0556.x>.
- Ngueleu, S. K., Rezanezhad, F., Al-Raoush, R. I., & Van Cappellen, P. (2018). Sorption of benzene and naphthalene on (semi)-arid coastal soil as a function of salinity and temperature. *Journal of Contaminant Hydrology*, 219, 61–71. <https://doi.org/10.1016/j.jconhyd.2018.11.001>.
- Ngueleu, S. K., Al-Raoush, R. I., Shafieiyoun, S., Rezanezhad, F., & Van Cappellen, P. (2019). Biodegradation kinetics of benzene and naphthalene in the vadose and saturated zones of a (semi)-arid saline coastal soil environment. *Geofluids*, 2019. <https://doi.org/10.1155/2019/8124716>.
- Ning, Z., Zhang, M., He, Z., Cai, P., Guo, C., & Wang, P. (2018). Spatial pattern of bacterial community diversity formed in different groundwater field corresponding to electron donors and acceptors distributions at a petroleum-contaminated site. *Water (Switzerland)*, 10, 1–14. <https://doi.org/10.3390/w10070842>.
- Pallud, C., Meile, C., Laverman, A. M., Abell, J., & Van Cappellen, P. (2007). The use of flow-through sediment reactors in biogeochemical kinetics: methodology and examples of applications. *Marine Chemistry*, 106, 256–271. <https://doi.org/10.1016/j.marchem.2006.12.011>.
- Perelo, L. W. (2010). Review: in situ and bioremediation of organic pollutants in aquatic sediments. *Journal of*

- Hazardous Materials*, 177, 81–89. <https://doi.org/10.1016/j.jhazmat.2009.12.090>.
- Rhykerd, L., Weaver, W., & McInnes, K. J. (1995). Influence of salinity on bioremediation oil in soil. *Environmental Pollution*, 90, 127–130. [https://doi.org/10.1016/0269-7491\(94\)00087-T](https://doi.org/10.1016/0269-7491(94)00087-T).
- Rushdi, A. I., Al-shaikh, I., El-mubarak, A. H., Alnaimi, H. A. J. A., Al-shamary, N., Hassan, H. M., & Abou, M. (2017). Characteristics and sources of anthropogenic and biogenic hydrocarbons in sediments from the coast of Qatar. *Marine Pollution Bulletin*, 124, 56–66. <https://doi.org/10.1016/j.marpolbul.2017.07.014>.
- Shafieiyoun, S., & Thomson, N. R. (2018). The role of intra-NAPL diffusion on mass transfer from MGP residuals. *Journal of Contaminant Hydrology*, 213, 49–61. <https://doi.org/10.1016/j.jconhyd.2018.04.002>.
- Shafieiyoun, S., & Thomson, N. R. (2019). Intra-NAPL diffusion and dissolution of a MGP NAPL exposed to persulfate in a flow-through system. *Journal of Hazardous Materials*, 365, 366–374. <https://doi.org/10.1016/j.jhazmat.2018.10.096>.
- Shafieiyoun, S., Thomson, N. R., Brey, A. P., Gasinski, C. M., Pence, W., & Marley, M. (2018). Realistic expectations for the treatment of FMGP residuals by chemical oxidants. *Journal of Contaminant Hydrology*, 219, 1–17. <https://doi.org/10.1016/j.jconhyd.2018.08.007>.
- Shafieiyoun, S., Al-Raoush, R. I., Ismail, R. E., Ngueleu, S. K., & Rezanezhad, F. (2020). Effects of dissolved organic phase composition and salinity on the engineered sulfate application in a flow-through system. *Environmental Science and Pollution Research*, 27, 11842–11854. <https://doi.org/10.1007/s11356-020-07696-6>.
- Shomar, B. (2015). Geochemistry of soil and groundwater in arid regions: Qatar as a case study. *Groundwater for Sustainable Development*, 1, 33–40. <https://doi.org/10.1016/j.gsd.2015.12.005>.
- Simpunanen, S., Dahl, M., Gerlach, M., Mikkonen, A., Malk, V., Mikola, J., & Romantschuk, M. (2016). Biostimulation proved to be the most efficient method in the comparison of in situ soil remediation treatments after a simulated oil spill accident. *Environmental Science and Pollution Research*, 25024–25038. <https://doi.org/10.1007/s11356-016-7606-0>.
- Sinke, A. J. C., Dury, O., & Zobrist, J. (1998). Effects of a fluctuating water table: column study on redox dynamics and fate of some organic pollutants. *Journal of Contaminant Hydrology*, 33, 231–246. [https://doi.org/10.1016/S0169-7722\(98\)00072-2](https://doi.org/10.1016/S0169-7722(98)00072-2).
- Stams, A. J. M., Plugge, C. M., de Bok, F. A. M., van Houten, B. H. G. W., Lens, P., Dijkman, H., & Weijma, J. (2005). Metabolic interactions in methanogenic and sulfate-reducing bioreactors. *Water Science and Technology*, 52, 13–20. <https://doi.org/10.2166/wst.2005.0493>.
- Suthersan, S., Houston, K., Schnobrich, M., & Horst, J. (2011). Engineered anaerobic bio-oxidation systems for petroleum hydrocarbon residual source zones with soluble sulfate application. *Ground Water Monitoring and Remediation*, 31, 41–46. <https://doi.org/10.1111/j.1745-6592.2011.01354.x>.
- Talbot, G., Topp, E., Palin, M. F., & Masse, D. I. (2008). Evaluation of molecular methods used for establishing the interactions and functions of microorganisms in anaerobic bioreactors. *Water Research*, 42, 513–537. <https://doi.org/10.1016/j.watres.2007.08.003>.
- Thamer, M., Al-kubaisi, A. R., Zahraw, Z., Abdullah, H. A., Hindy, I., & Khadium, A. A. (2013). Biodegradation of Kirkuk light crude oil by *Bacillus thuringiensis*, Northern of Iraq. *Natural Science*, 5, 865–873.
- The Interstate Technology and Regulatory Council (ITRC), 2011. Environmental Molecular Diagnostics Fact Sheets.
- Thierrin, J., Davis, G. B., Barber, C., Patterson, B. M., Pribac, F., Power, T. R., & Lambert, M. (1993). Natural degradation rates of BTEX compounds and naphthalene in a sulphate reducing groundwater environment. *Hydrological Sciences Journal*, 38, 309–322. <https://doi.org/10.1080/02626669309492677>.
- Vallejo, B., Izquierdo, A., Blasco, R., del Campo, P. P., & de Castro, M. D. L. (2001). Bioremediation of an area contaminated by a fuel spill. *Journal of Environmental Monitoring*, 3, 274–280. <https://doi.org/10.1039/b006402p>.
- Van De Graaf, A. A., Mulder, A., De Bruijn, P., Jetten, M. S. M., Robertson, L. A., & Kuenen, J. G. (1995). Anaerobic oxidation of ammonium is a biologically mediated process. *Applied and Environmental Microbiology*, 61, 1246–1251.
- Varjani, S. J. (2017). Microbial degradation of petroleum hydrocarbons. *Bioresource Technology*, 223, 277–286. <https://doi.org/10.1016/j.biortech.2016.10.037>.
- Ward, D. M., & Brock, T. D. (1978). Hydrocarbon biodegradation in hypersaline environments. *Applied and Environmental Microbiology*, 35, 353–359.
- Weber, W. J., & DiGiano, J. F. A. (1995). *Process dynamic in environmental systems*. New York: John Wiley & Sons Inc.
- Wei, Y., Thomson, N. R., Aravena, R., Marchesi, M., Barker, J. F., Madsen, E. L., Kolhatkar, R., Buscheck, T., Hunkeler, D., & DeRito, C. M. (2018). Infiltration of sulfate to enhance sulfate-reducing biodegradation of petroleum hydrocarbons. *Ground Water Monitoring and Remediation*. <https://doi.org/10.1111/gwmmr.12298>.
- Yigiterhan, O., Alföldy, B. Z., Giamberini, M., Turner, J. C., Al-Ansari, E. S., Abdel-Moati, M. A., Al-Maslamani, I. A., Kotb, M. M., Elobaid, E. A., Hassan, H. M., Obbard, J. P., & Murray, J. W. (2018). Geochemical composition of Aeolian dust and surface deposits from the Qatar Peninsula. *Chemical Geology*, 476, 24–45. <https://doi.org/10.1016/j.chemgeo.2017.10.030>.

Publisher's Note Springer Nature remains neutral with regard to jurisdictional claims in published maps and institutional affiliations.